Performance Analysis of Relay Model-based Energy Harvesting in CR-WBAN

Sree Nidhi SRINIVASAN, Pavithra SURESH KUMAR, Sridharan DURAISAMY

Dept. of ECE, Anna University, College of Engineering, Chennai, India

sreesvjsd@gmail.com, sanjuarumugam15@gmail.com, sridhar@annauniv.edu

Submitted November 16, 2024 / Accepted April 19, 2025 / Online first May 19, 2025

Abstract. *An emerging technique was introduced to extend the network lifetime of energy-limited relay nodes in wireless networks. In this paper, the spectral and energy efficiency of Wireless Body Area Networks (WBAN) is investigated. A novel Relay model-based WBAN with Energy Harvesting for enhancing spectrum utilization using Cognitive Radio (CR) technology. This approach involves the surrounding of RF signals, allowing the nodes to gather energy and process data within a WBAN, specifically for medical monitoring purposes enabling the coexistence of diverse implanted devices while maintaining their QoS. It facilitates the simultaneous operation of distinct sensor nodes for primary and secondary networks in on-body CR-WBAN, categorizing nodes based on medical and non-medical applications. The proposed protocols designed for energy harvesting notably Time Switching System (TSS) and Power-Splitting System (PSS) are utilized to enable the cooperation of secondary nodes with the primary network, allowing them to access the spectrum in exchange. The numerical analysis of proposed overlay CR-WBAN in aspects of outage probability, coverage analysis, throughput analysis, and energy efficiency performances considering a delay-limited scenario are examined. The numerical simulations confirm the validity of all the developed theoretical analyses and underscore the efficacy of the considered scheme by verifying using Monte Carlo simulations.*

Keywords

Wireless Body Area Networks (WBAN), Energy Harvesting (EH), Time Switching System (TSS), Power Splitting System (PSS), outage probability, cognitive radio

1. Introduction

The swift advancement of the Internet of Things has revolutionized various domains, driving transformative initiatives in intelligent urban centers, advanced industries, and innovative healthcare solutions [1]. Among these, healthcare stands out as a critical application area, particularly in addressing the challenges posed by an aging global population and the increasing prevalence of chronic illnesses. These challenges demand continuous medical monitoring and surveillance, which has led to the development of IoT-based Wireless Body Area Networks (WBANs) [2]. A WBAN consists of lightweight, cost-effective, compact-sized, portable, and less-power nodes that are implanted within the human body [3]. These nodes collect physiological data and wirelessly transmit it for real-time monitoring and analysis, playing a crucial role in regularly assessing patient health status. The implanted devices gather the data from nodes, transmit it to the AP/gateway and then forward it to the cloud for medical purposes [4]. Beyond healthcare, WBANs have found applications in diverse fields, including sports performance tracking, military operations, industrial automation, environmental monitoring, and even real-time gaming [5].

A key challenge in WBAN is the presence of low-power nodes, which results in reduced network performance and decreased link reliability. Designing a WBAN requires adhering to specific absorption rate (SAR) limits to prevent heart-related issues and potential tissue damage in the human body which can be affected by electromagnetic radiation [6]. So, it is necessary to transmit the power of sensor nodes at a low level to ensure safety. The network performance and link reliability in WBAN gradually decrease due to low power transmission and path loss [7–9].

One promising solution to the challenges of limited power capacity and path loss in WBANs is the integration of cooperative communication, which enhances the energy efficiency of sensor nodes. This approach is particularly critical for implanted nodes, where frequent battery replacement is not feasible due to practical and health-related constraints [10]. To further address energy limitations, researchers have explored various energy-scavenging interface circuits tailored for WBAN applications, each offering distinct levels of efficiency [11]. Among these techniques, energy harvesting from RF signals has emerged as a viable method to significantly reduce the power consumption of nodes, thereby extending the overall network lifetime [12–14].

Energy and spectrum harvesting techniques plays a pivotal role in addressing power constraints in WBANs. The methods for effectively managing power accumulation within nodes while optimizing spectrum utilization, offering a foundation for improving network performance. Building on this, cooperative communication has emerged as a prom-

DOI: 10.13164/re.2025.0353

ising strategy to optimize power allocation and reduce energy consumption in sensor nodes [15]. For instance, [16] examines the outage probability of transmissions across three scenarios—direct link, single relay system, and multi-relay system highlighting the benefits of cooperative approaches. Similarly, a space-time-coded network was introduced to enable fully cooperative communication through three configurations: direct link, Alamouti transmission, and cooperative networks. This technique demonstrated improved outage probability, error rates, and energy efficiency, particularly in low signal-to-noise ratio (SNR) conditions, compared to direct link scenarios [17]. Further advancements in power allocation strategies have been proposed, incorporating relay cooperation to maximize throughput in WBANs. The optimization framework addresses two key scenarios: one constrained by destination node power limits (DRL) and the other by relay power limits (RPL), utilizing time-switching and power-splitting protocols to enhance energy efficiency under varying conditions [18].

An energy-harvesting-aware WBAN has been proposed to enhance spectrum efficiency in communication links, leveraging both single-hop and dual-hop configurations for effective power management [19]. Additionally, a SWIPT-based two-way relay network employing a hybrid selection combining approach has been introduced to improve the robustness of communication channels [20]. To further optimize system performance, a joint power allocation strategy was suggested [21], utilizing the Maximal Ratio Combining (MRC) protocol. This approach, implemented with a time-switching protocol for both relay and direct link transmissions, significantly enhances system throughput.

In [22], a dynamic power-splitting technique was introduced to mitigate interference in nodes, aiming to maximize the ergodic rate while addressing delays in spectrum usage through cognitive radio. Similarly, studies [15–19] explored cooperative communication in WBANs, focusing on a two-tier architecture to enhance network performance. The challenges of sum-throughput maximization and spectrum utilization in WBAN systems for Simultaneous Wireless Information and Power Transfer (SWIPT) applications were tackled in [20] and [21]. While WBAN nodes can operate within the same frequency band, certain applications may demand more spectrum for specific nodes, creating situations where uniform allocation becomes detrimental to overall network performance.

In contrast to previous studies, we propose a novel CR-WBAN relay model with energy harvesting (EH) and a unique system design. We prioritize sensors based on their primary and secondary network, as certain nodes require increased energy and spectrum allocations for data transmission, which is facilitated through cognitive radio techniques. We also introduce additional performance metrics for the relay node in a secondary network with two secondary nodes. In this paper, the concept of cognitive radio is explored, with sensors utilized for both medical and non-medical applications. Nodes intended for medical purposes are given priority as primary users. This approach is geared towards guaranteeing a satisfactory quality-of-service (QoS) for these sensors.

We achieve this by facilitating the secondary sensor nodes. Additionally, this approach improves spectrum utilization efficiency, enabling a significant quantity of sensors to function within a similar frequency range. Moreover, the concept of utilizing RF-based energy harvesting can be investigated for achieving an ongoing energy supply. This is because the conventional methods of charging sensors or replacing their batteries are not feasible options. We utilize an overlay cognitive radio (CR) approach, which facilitates cooperation among secondary users while minimizing interference for primary users.

Additionally, the integration of radio signal-based energy harvesting into the proposed design ensures a consistent energy source for secondary users. The contributions arising from the proposed work: A novel EH-enabled overlay approach within a CR-WBAN framework, utilizing the Time-Switching System (TSS) and Power Splitting System (PSS) protocols. This protocol utilizes Amplify and Forward (AF) relay to improve communication among nodes, serving both medical and non-medical purposes.

In detail, we formulate a representation for the Outage Probability (OP) in the primary network, accounting for cases with and without spectrum access all while considering the existence of Direct Link (DL) communication. Furthermore, an analytical equation for the secondary network is developed. The findings highlight the significance of variables such as the spectrum access ratio and the TSS and PSS parameters in influencing the overall performance of our proposed design. The aim is to enhance notable improvements in spectral, energy efficiency and coverage area.

Figure 1 depicts the proposed architecture of the CR-WBAN. The sensor nodes are characterized by their compact size, low power, enhanced intelligence, and versatile placement options. They can be placed on the human body's surface, inserted within it, or used in conjunction with portable devices that individuals carry in different positions.

Sensor nodes in WBANs are capable of measuring various physiological attributes, including electroencephalograms (EEG), electrocardiograms (ECG), temperature, res-

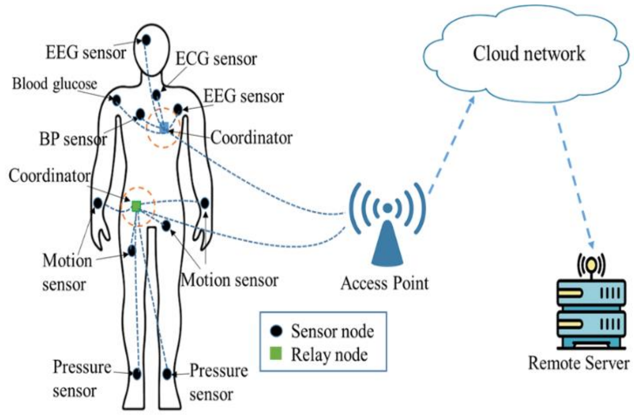

Fig. 1. Proposed CR-WBAN architecture.

piration rate, heart rate, and blood pressure, among others. These nodes gather critical physiological data and relay it to a coordinator, which then transmits the information wirelessly to a central server [23–25]. Users within the WBAN system are classified based on their application. Sensors used for medical diagnostics, such as EEG, ECG, and electromyography (EMG) sensors, are considered primary users due to their essential role in healthcare. Conversely, sensors used for non-medical purposes, such as motion and temperature sensors, are classified as secondary users. Spectrum sensing in real-world scenarios poses significant challenges, including (a) delays introduced during spectrum detection and (b) the infeasibility of spectrum sensing due to the constraints of low-power nodes. To address these issues, this research proposes the overlay paradigm of Cognitive Radio WBAN (CR-WBAN) for secondary users, ensuring seamless operation without interfering with primary users. The primary objectives of this paper are encapsulated in the following key aspects.

- The novel proposed work involves the implementation of CR-WBAN with energy harvesting with unique system model. This is accomplished by incorporating TSS and PSS protocols for spectrum access, enabling concurrent communication between primary and secondary users.
- About the primary network, we formulate expressions for the outage probability considering scenarios both with and without spectrum access, while accounting for DL transmission. Subsequently, we proceed with the derivation of the secondary network with outage probability expression.
- We delve into an analysis of the throughput, energy efficiency, and coverage analysis. This examination is conducted for both TSS and PSS protocols, all within the context of a scenario with limitations on delay.
- The outcomes of our investigation showcase how the spectrum access factor, as well as the parameters associated with the TSS and PSS protocols, influence the overall performance of the CR-WBAN with EH. These findings offer valuable insights that can serve as guidelines for designing practical WBANs to attain high spectral and coverage analysis.

The paper is structured as follows: Section 2 presents the mathematical model of the proposed system. Section 3 analyzes the outage probability of the primary and secondary networks, as well as the performance analysis of the proposed system, through analytical derivations. Numerical results and discussions are provided in Sec. 4, followed by concluding remarks in Sec. 5.

2. System Description

Figure 2 represents the analytical model of cognitive radio in WBAN with Energy Harvesting (EH), considering both primary and secondary users within the network. The primary network is composed of a transmitting node, referred to as A, and a receiving node, referred to as B. Conversely, the secondary network is comprised of a transmitting node, referred to as D, that operates under energy constraints, and its corresponding receiving nodes, denoted as C and E. Node A are in direct link to node B and simultaneously considering the possibility of utilizing the secondary node D as a relay to facilitate their communication.

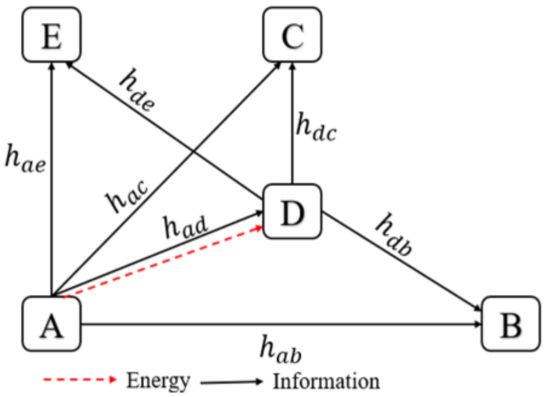

Fig. 2. Analytical representation of CR-WBAN.

Nevertheless, the assumption is made that node D operates with limited energy resources. Consequently, from primary transmissions node D harvests its energy initially and subsequently employs this harvested energy to operate as a relay for the primary signal, concurrently transmitting its signal. The assumptions in the proposed protocol are given below.

- The assumption is made that the CR-WBAN is stationary inside a closed room, isolated from any devices of interference. In addition, each sensor is fitted with a single antenna, which is necessary because of their restricted size, and they function in a half-duplex scheme.
- The proposed protocols are TSS and PSS for enabling energy harvesting and information transmission at energy limited in relaying networks.
- The secondary node D can perform energy harvesting using radio frequencies. Its function is to operate as a relay for the primary network through the utilization of the AF technique. Simultaneously, it employs the primary spectrum for its individual transmission purposes.
- The noise that exists is described as Additive White Gaussian Noise (AWGN) with a mean of zero and a variance of N_0.
- Each link in the network is susceptible to log-normal fading, also h_{ij} is the gain of the channel from node i to node j, where $i \in$ {a, d}, and $j \in$ {b, d, c, e}, ensuring that $i \neq j$. It holds significance to consider the log-normal distribution for capturing the large-scale fading characteristics observed in WBAN.
- T is the block time in which a certain block of information is transmitted. A_a and A_d indicate the transmission powers at nodes A and D.

The secondary node D can utilize RF-based energy harvesting for spectrum access with primary users by prioritizing cooperation with primary transmissions. To achieve this, we examine two protocols for spectrum access systems based on energy harvesting namely TSS and PSS for the suggested CR-WBAN, as detailed in the following sections.

2.1 TSS Protocol

The TSS protocol utilizes half-duplex operation and divides the block time into three sub-blocks with $\alpha \in (0,1)$. From primary signal node A to harvest energy with time of αT and it allocates time for broadcasting information $(1-\alpha)T$. At nodes D, B, C, and E $(1-\alpha)T/2$ time is dedicated to receiving data from node A. Meanwhile, during the remaining time of $(1-\alpha)T/2$, the transmission of a network-coded message from node D to nodes B, C, and E takes place. Therefore, the expression for the harvested energy at node D is as follows.

$$E_{\mathrm{d}} = \Theta A_{\mathrm{a}} \left|h_{\mathrm{ad}}\right|^2 \alpha T \,. \tag{1}$$

The energy conversion efficiency, represented by Θ, within the range of (0,1), depends on both the energy harvesting (EH) circuitry and rectification process employed. As a result, the transmission power of node D in the duration of $(1-\alpha)T/2$ is as follows.

$$P_{\mathrm{d}} = \frac{E_{\mathrm{d}}}{(1-\alpha)T/2} = \frac{2\alpha\Theta A_{\mathrm{a}}\left|h_{\mathrm{ad}}\right|^2}{(1-\alpha)}. \tag{2}$$

In the period of the second sub-block transmission slot, node A sends an informational signal x_{a} to node B through broadcasting. The secondary nodes D, C, and E also receive this signal. Here $j \in \{\mathrm{b, d, c, e}\}$, and $n_{\mathrm{a}j}$ represents the AWGN variable. Consequently, the received signal y_{ab}, y_{ad}, y_{ac} and y_{ae} at nodes B, D, C and E respectively, is given as

$$y_{\mathrm{a}j} = \sqrt{A_{\mathrm{a}}}\, h_{\mathrm{a}j} \cdot x_{\mathrm{a}} + n_{\mathrm{a}j}. \tag{3}$$

During the transmission phase within the third sub-block, node D participates in aiding the primary data communication through an AF relaying cooperation. Simultaneously, node D also broadcasts with its receiver nodes C and E. To enable the AF relaying cooperation, node D divides its harvested power, denoted as A_{d}. To perform three transmissions such as node D allocates a portion of its harvested power ζA_{d} to form the relayed transmission of the primary signal component x_{a} to node B and node D allocates the power of $(1-\zeta)A_{\mathrm{d}}/2$ to transmit the secondary signal component x_{d} to node C and E. In the CR-WBAN, the power allocation factor $\zeta \in (0,1)$ to spectrum access, which is expressed as follows

$$x_{\mathrm{s}} = \sqrt{\varsigma}\, A_{\mathrm{d}} \frac{y_{\mathrm{ad}}}{\sqrt{\left|y_{\mathrm{ad}}\right|^2}} + 2\sqrt{\frac{(1-\varsigma)\,A_{\mathrm{d}}}{2}} \cdot x_{\mathrm{d}}. \tag{4}$$

In the third sub-block phase, signals received from node D at nodes B, C and E implied as y_{db}, y_{dc} and y_{de} respecttively, can be expressed as follows

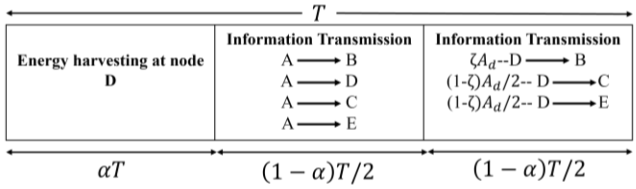

Fig. 3. Transmission block for TSS protocol.

$$y_{\mathrm{d}j} = h_{\mathrm{d}j}\ x_{\mathrm{s}} + n_{\mathrm{d}j} \tag{5}$$

where $j \in \{\mathrm{b, c, e}\}$ and $n_{\mathrm{d}j}$ represents the AWGN variable. Regarding the primary user, the instantaneous SNR at node B via direct communication is given by

$$y_{\mathrm{ab}} = \eta_{\mathrm{a}} \left|h_{\mathrm{ab}}\right|^2 \tag{6}$$

where $\eta_{\mathrm{a}} = A_{\mathrm{a}} / N_0$ is the transmission SNR, at the same time end to end SNR at B through the relay link in the TSS protocol can be represented using (2) and (5) as follows.

$$y_{\mathrm{adb}} = \frac{\zeta\gamma_{\mathrm{ad}}\beta\left|h_{\mathrm{db}}\right|^2}{2(1-\zeta)\gamma_{\mathrm{ad}}\beta\left|h_{\mathrm{db}}\right|^2 + \zeta\beta\left|h_{\mathrm{db}}\right|^2 + 1} \tag{7}$$

where $\gamma = \eta_{\mathrm{a}}|h_{\mathrm{ad}}|^2$ and $\beta = 2\alpha\Theta/(1-\alpha)$. For the secondary network, the signal is captured at node C of the primary signal component x_{a}. This noise within the received primary signal can be leveraged earlier during the transmission phase within the second sub-block and the interference can be eliminated at node C [26]. The SNR at node C after the process can be shown as follows.

$$\gamma_{\mathrm{adc}} = \frac{2(1-\zeta)\gamma_{\mathrm{ad}}\beta\left|h_{\mathrm{dc}}\right|^2}{\zeta\beta\left|h_{\mathrm{dc}}\right|^2 + 1}. \tag{8}$$

The SNR at node E from the node D which is another node of the secondary user's network is given by

$$\gamma_{\mathrm{ade}} = \frac{2(1-\zeta)\gamma_{\mathrm{ad}}\beta\left|h_{\mathrm{de}}\right|^2}{\zeta\beta\left|h_{\mathrm{de}}\right|^2 + 1}. \tag{9}$$

2.2 PSS Protocol

In the PSS protocol, the total transmission time T is divided into two sub-blocks, employing a half-duplex scheme. In this block, half of the allocated time is utilized for primary users, while another half is assigned for secondary users, as illustrated in Fig. 4. At the onset of the transmission phase, node A emits a signal with unit energy labeled as x_{a}. Consequently, the signal received at nodes B, D, C, and E are represented as y_{ab}, y_{ad}, y_{ac} and y_{ae} respectively can be expressed as follows

$$y_{\mathrm{a}j} = \sqrt{A_{\mathrm{a}}}\, h_{\mathrm{a}j} x_{\mathrm{a}} + n_{\mathrm{a}j}. \tag{10}$$

Received signal y_{ad} is divided into two components, denoted by $\sqrt{\rho}\, y_{\mathrm{ad}}$ and $\sqrt{(1-\rho)}\, y_{\mathrm{ad}}$, where the power splitting ratio is ρ $(0 \le \rho \le 1)$. The first component is utilized to harvest energy for recharging the battery, while the second component is employed for information transmission. Con-

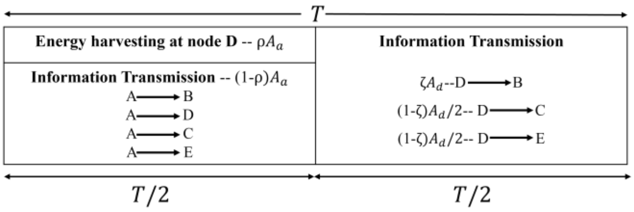

Fig. 4. Transmission block for PSS protocol.

sequently, the signal received at the energy harvesting input is given as described above, considering the possible values of $j \in \{\mathrm{b,d,c,e}\}$ and the presence of AWGN represented by n_{aj}.

$$\sqrt{\rho}\, y_{\mathrm{ad}} = \sqrt{\rho A_{\mathrm{a}}}\, h_{\mathrm{ad}} x_{\mathrm{a}} + \sqrt{\rho}\, n_{\mathrm{ad}}. \tag{11}$$

From (11), the energy harvested at D is expressed as

$$E_{\mathrm{d}} = \frac{\Theta \rho A_{\mathrm{a}} \left|h_{\mathrm{ad}}\right|^2 T}{2}. \tag{12}$$

The energy conversion efficiency ($0 \le \Theta \le 1$) of the inverter circuitry at D is considered, and the noise statistic is disregarded [31]. Our focus is on the harvested energy with $A_{\mathrm{d}} << A_{\mathrm{a}}$. For the remaining $T/2$ time the power distributed is expressed as

$$P_{\mathrm{d}} = \frac{E_{\mathrm{d}}}{T/2}. \tag{13}$$

The expression can be further represented using (12) as

$$P_{\mathrm{d}} = \Theta \rho A_{\mathrm{a}} \left|h_{\mathrm{ad}}\right|^2. \tag{14}$$

Conversely, the information receiver (IR) at point D receives the base-band signal as follows:

$$\begin{aligned} Y_{\mathrm{AD}} &= \sqrt{(1-\rho)}\, y_{\mathrm{ad}} = \\ &\sqrt{(1-\rho) A_{\mathrm{a}}}\, h_{\mathrm{ad}} x_{\mathrm{a}} + \sqrt{(1-\rho)}\, n_{\mathrm{ad}} + n_{\mathrm{RF}}. \end{aligned} \tag{15}$$

In this context, n_{RF} signifies the sampled AWGN that emerges from the conversion of RF to baseband signal. The expression for the total AWGN noise at IR is calculated as $n_{\mathrm{AD}} = \sqrt{(1-\rho)}\, n_{\mathrm{ad}} + n_{\mathrm{RF}}$. During the second block of transmission, node D acts as an AF relay to enable the primary user operations, also communication with its dedicated receiver C and E at the same time. Consequently, in the first phase, node D amplifies and then sends the signal received at IR to node B, concurrently transmitting its information signal x_{d}, to nodes C and E. During this simultaneous transmission, node D utilizes advanced signal processing methods to divide its harvested power A_{d} using the spectrum access factor $\zeta \in (0, 1)$. This allows it to overlay its signal x_{d} with Y_{ad}, resulting in the combined signal being given by

$$x_{\mathrm{s}} = \sqrt{\varsigma A_{\mathrm{d}}}\, \frac{Y_{\mathrm{AD}}}{\sqrt{\left|Y_{\mathrm{AD}}\right|^2}} + 2\sqrt{\frac{(1-\varsigma) A_{\mathrm{d}}}{2}}\, x_{\mathrm{d}}. \tag{16}$$

Consequently, the signals that nodes B, C, and E have received from D during the sub-block are labeled as y_{db}, y_{dc} and y_{de}, respectively, and can be expressed as follows

$$y_{\mathrm{d}j} = h_{\mathrm{d}j} x_{\mathrm{s}} + n_{\mathrm{d}j} \tag{17}$$

where $j \in \{\mathrm{b, c, e}\}$ and $n_{\mathrm{d}j}$ is the AWGN. Hence, the SNR at point B through the direct link in primary communication can be expressed from (10) as

$$\gamma_{\mathrm{ab}} = \eta_{\mathrm{a}} \left|h_{\mathrm{ab}}\right|^2. \tag{18}$$

Formulating the SNR at point B, transmitted through the relay link, involves utilizing (14) to (17) as

$$\gamma_{\mathrm{adb}} = \frac{\zeta \gamma_{\mathrm{ad}} \delta \left|h_{\mathrm{db}}\right|^2}{2(1-\zeta)\gamma_{\mathrm{ad}} \delta \left|h_{\mathrm{db}}\right|^2 + \zeta \varrho \left|h_{\mathrm{db}}\right|^2 + 1} \tag{19}$$

where $\delta = \Theta\rho$ and $\varrho = \Theta\rho/(1-\rho)$. In terms of secondary communication, we can infer from (17) that the signal received at node C includes a primary signal component x_{s}, which functions as interference. However, this interference is eliminated [27] by employing the primary signal decoded during the initial transmission phase. As a result, we can express the instantaneous SNR at C as follows.

$$\gamma_{\mathrm{adc}} = \frac{2(1-\zeta)\gamma_{\mathrm{ad}} \delta \left|h_{\mathrm{dc}}\right|^2}{\zeta \varrho \left|h_{\mathrm{dc}}\right|^2 + 1}. \tag{20}$$

The noise statistics at the relay can be eliminated from SNR expressions (19) and (20). The SNR at node E of the secondary user is given by

$$\gamma_{\mathrm{ade}} = \frac{2(1-\zeta)\gamma_{\mathrm{ad}} \delta \left|h_{\mathrm{de}}\right|^2}{\zeta \varrho \left|h_{\mathrm{de}}\right|^2 + 1}. \tag{21}$$

3. Performance Analysis

We assess the CR-WBAN performance utilizing two protocols, namely TSS and PSS protocol. The performance analysis will involve evaluating various key metrics to assess the coverage distance, energy efficiency, and throughput of each protocol in the CR-WBAN. We assess how the overall performance of the CR-WBAN using the PSS parameter ρ, TSS parameter α, and power splitting factor ζ. Continuing the analysis, we start by providing the statistical details of the relative fading channels. Taking into account the log-normal fading for WBAN, we can represent the Probability Density Function (PDF) and Cumulative Distribution Function (CDF) of $|h_{ij}|^2$, where $i \in \{\mathrm{a, d}\}$ and $j \in \{\mathrm{b, d, c, e}\}$ with $i \neq j$, as follows, respectively, by [19], [32]

$$f_{\left|h_{ij}\right|^2}(x) = \frac{1}{2\sqrt{2\pi}\sigma_{ij}\, x} \exp\left(-\left(\frac{\ln(x) - 2\mu_{ij}}{2\sqrt{2}\sigma_{ij}}\right)^2\right), \tag{22}$$

and

$$F_{\left|h_{ij}\right|^2}(x) = \frac{1}{2}\left(1 + \mathrm{erf}\left(\frac{\ln(x) - 2\mu_{ij}}{2\sqrt{2}\sigma_{ij}}\right)\right). \tag{23}$$

The above-mentioned parameter μ_{ij} is the mean and σ_{ij} is the standard deviation, while $\mathrm{erf}(\cdot)$ denotes the standard error function.

3.1 Outage Probability of Primary Network

Concerning the primary network, we analyze the OP in scenarios both with and without spectrum access, while taking into account the existence of direct link communication (A→B). Subsequently, we then proceed to perform an analysis OP of the primary network, covering both the TSS and PSS protocols. R_p signifies the target rate designated for the primary user and R_s represents the target rate assigned to the secondary user. To achieve this, we can represent their corresponding SNRs from (7) and (19) in a standardized form as follows:

$$\gamma_{\mathrm{adb}} = \frac{\zeta \gamma_{\mathrm{ad}} \beta_1 |h_{\mathrm{db}}|^2}{2(1-\zeta)\gamma_{\mathrm{ad}} \beta_1 |h_{\mathrm{db}}|^2 + \zeta \beta_2 |h_{\mathrm{db}}|^2 + 1} \tag{24}$$

with $\beta_1 = \beta_2 = 2\alpha\phi / (1 - \alpha)$ for TSS protocol, whereas $\beta_1 = \Theta\rho$ and $\beta_2 = \Theta\rho / (1 - \rho)$ for PSS protocol.

a) Direct Link (DL) Communication

Provided target rate R_p, we examine the OP of the primary network when utilizing direct communication without spectrum access is expressed as

$$\begin{aligned} \gamma_{\mathrm{a}} &= \log_2(1+\gamma_{\mathrm{ab}}), \\ P_{\mathrm{out}}^{\mathrm{DL}}(R_{\mathrm{p}}) &= \Pr[\gamma_{\mathrm{a}} < R_{\mathrm{p}}]. \end{aligned} \tag{25}$$

The significance that the DL transmission relies on a transmission phase from node A to node B further explained as

$$P_{\mathrm{out}}^{\mathrm{DL}}(R_{\mathrm{p}}) = F_{\gamma_{\mathrm{ab}}}(\gamma'_{\mathrm{a}}) \tag{26}$$

where $\gamma'_{\mathrm{a}} = 2^{R_{\mathrm{p}}} - 1$. By applying a random variable transformation, we can derive the expression for the CDF $F_{\gamma_{ab}}(x)$ from (23):

$$F_{\gamma_{\mathrm{ab}}}(x) = \frac{1}{2}\left(1 + \operatorname{erf}\left(\frac{\ln(x) - \ln(\eta_{\mathrm{a}}) - 2\mu_{\mathrm{ab}}}{2\sqrt{2}\sigma_{\mathrm{ab}}}\right)\right). \tag{27}$$

Hence, if we substitute $x = \gamma'_a$ into the CDF $F_{\gamma_{ab}}(x)$ derived in (27), we can calculate the necessary OP of DL transmission on this evaluation.

b) Spectrum Access Cooperation with DL Transmission

To achieve a target rate R_{p}, the OP of the primary network in CR-WBAN employing the TSS/PSS protocol can be represented using MRC. This involves utilizing (6) or (18) and (24) in the expression:

$$\begin{aligned} P_{\mathrm{out}}^{\mathrm{Pri}}(R_{\mathrm{p}}) &= \Pr\left[\frac{1}{\tau}\log_2(1+\gamma_{\mathrm{ab}}+\gamma_{\mathrm{adb}}) < R_{\mathrm{p}}\right] = \\ &\Pr[\Lambda_{\mathrm{a}} < \gamma_{\mathrm{a}}] = F_{\Lambda_{\mathrm{a}}}(\gamma_{\mathrm{a}}). \end{aligned} \tag{28}$$

$\Lambda_{\mathrm{a}} = \gamma_{\mathrm{ab}} + \gamma_{\mathrm{adb}}$ and $\gamma_{\mathrm{a}} = 2^{\tau R_{\mathrm{p}}} - 1$, where $\tau = 2$ for the PSS protocol and $\tau = 2/(1 - \alpha)$ for TSS protocol (28) it is reformulated as

$$\begin{aligned} F_{\Lambda_{\mathrm{a}}}(\gamma_{\mathrm{a}}) &= \Pr[(\gamma_{\mathrm{ab}} + \gamma_{\mathrm{adb}}) < \gamma_{\mathrm{a}}], \\ A1 &= \int_0^{\gamma_{\mathrm{a}}}\int_0^{\gamma_{\mathrm{a}}-y} f_{\gamma_{\mathrm{adb}}}(x) f_{\gamma_{\mathrm{ab}}}(y)\,\mathrm{d}x\,\mathrm{d}y. \end{aligned} \tag{29}$$

Additionally, by employing an M-step staircase approximation method [28] for the triangular integral region involved in (29), we can express A1 as follows

$$A1 = \sum_{i=0}^{M-1}\left\{F_{\gamma_{\mathrm{ab}}}\left(\frac{i+1}{M}\gamma_{\mathrm{a}}\right) - F_{\gamma_{\mathrm{ab}}}\left(\frac{i}{M}\gamma_{\mathrm{a}}\right)\right\} \times F_{\gamma_{\mathrm{adb}}}\left(\frac{M-i}{M}\gamma_{\mathrm{a}}\right).$$

Theorem 1: The CDF of the CR-WBAN with the TSS/PSS protocol, considering log-normal fading channels, can be represented as

$$F_{\gamma_{\mathrm{adb}}}(x) = \begin{cases} 1, & \text{if } x \geq \dfrac{\zeta}{1-\zeta}; \\ \phi(x), & \text{if } x < \dfrac{\zeta}{1-\zeta} \end{cases} \tag{30}$$

$$\begin{aligned} \phi(x) = \int_0^{\infty} \frac{1}{2}\left(1 + \operatorname{erf}\left(\frac{\ln\left(\dfrac{x(1+\zeta\beta_2 y)}{\beta_1(\zeta - (1-\zeta)x)y}\right) - 2\mu_{\mathrm{ad}}}{2\sqrt{2}\sigma_{\mathrm{ad}}}\right)\right) \times \\ \frac{1}{2\sqrt{2}\sigma_{\mathrm{db}} y}\exp\left(-\left(\frac{\ln(y) - 2\mu_{\mathrm{db}}}{2\sqrt{2}\sigma_{\mathrm{db}}}\right)^2\right)\mathrm{d}y. \end{aligned} \tag{31}$$

Proof: it is detailed in Appendix A

From the condition $x < \zeta / (1 - \zeta)$ it allows the relay cooperation given in (30), the CDF implies the secondary communication in CR-WBAN.

3.2 Outage Probability of Secondary Network

The SNR at node C, the performance of the secondary network for TSS and PSS protocols from (8) and (20) is given by

$$\gamma_{\mathrm{adc}} = \frac{2(1-\zeta)\gamma_{\mathrm{ad}}\beta_1 |h_{\mathrm{dc}}|^2}{\zeta\beta_2 |h_{\mathrm{dc}}|^2 + 1}. \tag{32}$$

The SNR at node E for the secondary network for TSS and PSS protocol from (9) and (21) is given by

$$\gamma_{\mathrm{ade}} = \frac{2(1-\zeta)\gamma_{\mathrm{ad}}\beta_1 |h_{\mathrm{de}}|^2}{\zeta\beta_2 |h_{\mathrm{de}}|^2 + 1}. \tag{33}$$

$\beta_1 = \beta_2 = 2\alpha\phi / (1 - \alpha)$ for TSS protocol and $\beta_1 = \beta_2 = \phi\rho / (1 - \rho)$ for PSS protocol. The secondary communication of OP for target rate R_{s} is given by

$$\begin{aligned} \gamma_{\mathrm{d}} &= \frac{1}{\tau}\log_2(1+\gamma_{\mathrm{adc}}+\gamma_{\mathrm{ade}}), \\ P_{\mathrm{out}}^{\mathrm{sec}}(R_{\mathrm{s}}) &= \Pr[\gamma_{\mathrm{d}} < R_{\mathrm{s}}] = \Pr[(\gamma_{\mathrm{adc}}+\gamma_{\mathrm{ade}}) < \gamma_{\mathrm{s}}] = F_{\Lambda_{\mathrm{s}}}(\gamma_{\mathrm{s}}). \end{aligned} \tag{34}$$

$\Lambda_{\mathrm{s}} = \gamma_{\mathrm{adc}} + \gamma_{\mathrm{ade}}$, $\gamma_{\mathrm{s}} = 2^{\tau R_{\mathrm{s}}} - 1$, where $\tau = 2/(1 - \alpha)$ for TSS protocol and $\tau = 2$ for the PSS protocol. $P_{\mathrm{out}}^{\mathrm{sec}}(R_{\mathrm{s}})$ for secondary communication is evaluated in CDF $F_{\gamma_{\rm acd}}(x)$ and is expressed as in theorem 2. The M- step staircase for (32) is $\sum_{i=0}^{M-1}\Delta F_i\, f\left(\frac{i+1}{M}|h_{\rm dc}|^2\right)$, where ΔF_i is the change in CDF between two points, and $f(|h_{\rm dc}|^2)$ is the integrand derived from $\gamma_{\rm adc}$. M and N are the number of steps in the M-step staircase approximation.

Theorem 2: The CDF of the CR-WBAN with the TSS/PSS protocols, considering log-normal fading channels, can be represented as $F_{\gamma_{\rm adc}}(x)$

$$F_{\Lambda_s}(x)= \int_0^\infty \frac{1}{2}\left(1+\mathrm{erf}\left(\frac{\ln\left(\frac{x(1+\zeta\beta_2 y)}{\beta_1(1-\zeta)y}\right)-2\mu_{\rm ad}}{2\sqrt{2}\sigma_{\rm ad}}\right)\right)\times \frac{1}{2\sqrt{2}\sigma_{\rm dc}y}\exp\left(-\left(\frac{\ln(y)-2\mu_{\rm dc}}{2\sqrt{2}\sigma_{\rm dc}}\right)^2\right)\times \frac{1}{2\sqrt{2}\sigma_{\rm de}y}\exp\left(-\left(\frac{\ln(y)-2\mu_{\rm de}}{2\sqrt{2}\sigma_{\rm de}}\right)^2\right)\mathrm{d}y. \tag{35a}$$

Proof: it is provided in Appendix B.

From (35a) $x = \gamma_{\rm d}$ which can determine $P_{\rm out}^{\rm sec}(R_{\rm s})$ for the target rate $R_{\rm s}$. The OP for the secondary network is obtained. The close form of (35b), using Chebyshev–Gauss quadrature, in terms of N nodes $t_i = \cos((2i-1)/(2N)\pi)$. t_i is the Chebyshev–Gauss quadrature node or the discrete step in the M-step staircase approach.

$$F_{\Lambda_s}(x)=\frac{\pi}{N}\sum_{i=1}^{N}\frac{1}{2}\left(1+\mathrm{erf}\left(\frac{\ln\left(\frac{x\left(1+\zeta\beta_2\frac{1+t_i}{1-t_i}\right)}{\beta_1(1-\zeta)\frac{1+t_i}{1-t_i}}\right)-2\mu_{\rm ad}}{2\sqrt{2}\sigma_{\rm ad}}\right)\right) \frac{1}{2\sqrt{2}\sigma_{\rm dc}\frac{1+t_i}{1-t_i}}\exp\left(-\left(\frac{\ln\left(\frac{1+t_i}{1-t_i}\right)-2\mu_{\rm dc}}{2\sqrt{2}\sigma_{\rm dc}}\right)^2\right)\times \frac{1}{2\sqrt{2}\sigma_{\rm de}\frac{1+t_i}{1-t_i}}\exp\left(-\left(\frac{\ln\left(\frac{1+t_i}{1-t_i}\right)-2\mu_{\rm de}}{2\sqrt{2}\sigma_{\rm de}}\right)^2\right)\mathrm{d}y. \tag{35b}$$

3.3 Constrained Power Distribution Policy for Spectrum Access

Focusing on the power allocation factor for spectrum access at the secondary node D, we can determine a suitable value for ζ that ensures the QoS requirement of the primary network is considered. From (30) the power allocation factor is determined based on the condition $\gamma_{\rm a} < \zeta / (1-\zeta)$ for predetermined threshold $\gamma_{\rm a}$ of the primary network as,

$$\frac{\gamma_a}{1-\gamma_a} < \zeta < 1 \cdot \tag{36}$$

However, from (28), it is evident that $\gamma_{\rm a}$ is influenced by both $R_{\rm p}$ and τ. Therefore, while employing the spectrum access condition for the TSS protocol, our initial stage includes computing the TSS parameter α value for attaining a minimal OP, as discussed in Sec. 4. Subsequently, with this determined value of α, we proceed to calculate the effective value of ζ to implement a spectrum access system. Additionally, it is important to reduce the value of ζ for increased spectrum access to secondary networks access.

3.4 Throughput Analysis

It encompasses the computation of throughput under latency constraints, which is crucial for assessing performance and evaluating spectrum utilization in CR-WBAN. Mean spectral efficiency is also known as wireless system-based cooperative communication. The throughput under the latency constraint is specified as the rate of transmission that can be ensured across all fading conditions, while also meeting specific delay limits, without relying on the extended long-term behavior [30].

In CR-WBAN, the latency-constrained throughput can be represented as the combined value of specific target rates for both primary and secondary communication systems to meet their respective data rate requirements while adhering to the given latency constraints. The network throughput which can be effectively achieved over log-normal fading channels is formulated according to the obtained equations for the OP. Expanding on the obtained formulations for the OP, we can express the network throughput as

$$S_{\rm T} = \frac{1}{\tau}\left[(1-P_{\rm out}^{\rm Pri}(R_{\rm p}))R_{\rm p} + (1-P_{\rm out}^{\rm sec}(R_{\rm s}))R_{\rm s}\right] \tag{37}$$

where $P_{\rm out}^{\rm sec}(R_{\rm s})$ and $P_{\rm out}^{\rm Pri}(R_{\rm p})$ express the OP measures achieved in the preceding subsections for both primary and secondary users. In (37), when we assign $R_{\rm p} = R_{\rm s} = R$, the maximum achievable system throughput $S_{\rm T}$ can be expressed as $S_{\rm T} = 2R/\tau$.Therefore, depending on the value of τ, we can easily determine the value of R is equivalent to the maximum throughput system determined for the PSS protocol, whereas, for the TSS protocol, it is $R(1-\alpha)$.

3.5 Energy Efficiency

Derived from the throughput formulation provided in (37), we conduct an evaluation of the energy efficiency of the investigated EH-based CR-WBAN. This analysis holds significant implications as it can assist in the design of EH-based CR-WBAN for prolonging the lifetime of the network.

In essence, the ratio of total data delivered to total energy consumed is used to measure the system's energy efficiency [33]. For the TSS protocol, the total energy used by the primary user A accounts for the absolute energy debilitated in the network during the initial sub-block EH phase and energy debilitated in the second transmission block. The energy obtained by secondary node D during the first sub-block energy harvesting phase is equal to the energy used during the third sub-block transmission phase:

$$\begin{cases} \dfrac{S_{\mathrm{T}}}{\dfrac{Aa}{2}(1+\alpha)}, \text{for TSS protocol;} \\ \dfrac{S_{\mathrm{T}}}{\dfrac{Aa}{2}}, \qquad\quad \text{for PSS protocol.} \end{cases} \tag{38}$$

Hence, the energy efficiency equation for the examined CR-WBAN (37) within constrained delay can be formulated as the quotient of the overall data transmission as indicated in (37) and the overall energy consumed within the network.

3.6 Coverage Analysis

The coverage area within the network for the proposed work is analyzed. We analyze the proposed method on spectrum coverage. The evaluation of coverage for the standard cooperative diversity system has been factored in [29]. Cell coverage is linked to the likelihood of signal outage, this is defined as the largest distance from the center of a cell within which the signal strength in the covered region surpasses a designated threshold SNR with a probability not lesser than $1 - P_{\mathrm{out}}$. In the subsequent examination, $d_1 = d_2 \simeq d_0/2$. Thus, by using (39), we can deduce that the largest permissible distance d must fulfill the subsequent equation.

$$d_0 = \left[\frac{2^{\alpha K+1} P\, P_{\mathrm{out}}\, R_{\mathrm{p}}}{(\zeta_i^K(R_{\mathrm{p}}) + \zeta_i^K(R_{\mathrm{p}}/2) R_{\mathrm{p}})} \right]^{\frac{1}{\alpha(K+1)}}. \tag{39}$$

4. Numerical Results and Discussion

Our objective is to showcase the assessment of the CR-WBAN performance employing both the TSS and PSS protocols. We achieve this by conducting numerical investigations through Monte Carlo simulations. Utilizing the attributes of the CR-WBAN, this section utilizes the parameters, the primary transmit power $A_{\mathrm{a}} = 1$ mW, $\Theta = 0.7$ is energy conversion efficiency, and the block time for transmission $T = 1$ ms is executed by log-normal fading distribution, from [24] relates to the configuration of the CR-WBAN where specific node arrangements are made including A positioned on the chest, B on the right arm, C placed on the left leg, D at the center waist, and E on the right leg, as given in Tab. 1.

μ_{ij},σ_{ij}	**Right arm (B)**	**Center waist (D)**	**Left leg (C)**	**Right leg (E)**
Chest (A)	–2.58, 4.89	–0.88, 2.96	–1.62, 3.47	–1.58, 3.89
Center waist (D)	–0.28, 1.34	--	–0.92, 2.74	–0.76, 2.14

Tab. 1. Parameters of log-normal distribution for CR-WBAN.

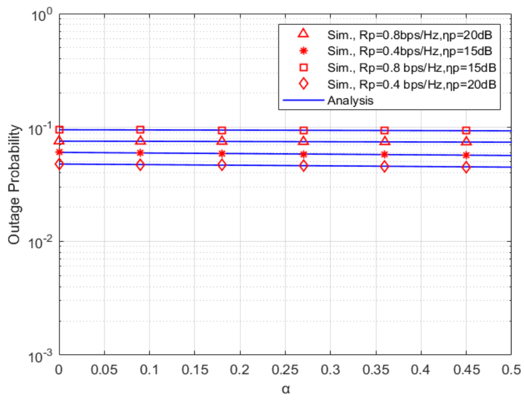

Fig. 5. OP vs α for TSS protocol in the primary network.

Analytical OP curves for primary and secondary networks are derived using (28), (35a), and (35b) respectively, with $M = 50$ for accuracy, implemented in MATHEMATICA. Monte Carlo simulations are conducted in MATLAB software to validate the analytical results. All figures demonstrate good agreement between analytical and simulation curves.

Figure 5 demonstrates the TSS parameter α with the performance of outage probability for the primary network within the CR-WBAN for various sets of target rate R_{p} and η_{p} SNR values. Thus, we select the values of $\alpha = 0.2$ and $\zeta = 0.8$ that ensure they satisfy the spectrum access condition $\gamma_{\mathrm{a}}(1 + \gamma_{\mathrm{a}}) < \zeta < 1$ are discussed in Sec. 3. Through an analysis of the variety of curves illustrated in this figure, we identify the critical value of α that minimizes the OP. To facilitate spectrum access cooperation, $\zeta = 0.8$ is found to effective value. The analysis in the simulated plots represents the results obtained from the theoretical model, which were derived analytically to validate the simulation outcomes. The outage probability reflects the performance of the proposed system under stringent conditions, such as low-power nodes and challenging propagation environments. While this may be high for certain critical WBAN applications, such as real-time medical monitoring, it is an intermediate result that highlights the trade-offs between power efficiency and reliability. Further optimization, such as employing advanced relay cooperation strategies, can significantly reduce the outage probability in practical scenarios, thereby enhancing reliability for critical applications.

Figure 6 illustrates the OP vs SNR curves for the TSS protocol for the primary network. These curves are plotted for different target rates ($R_{\mathrm{p}} = 0.4$, 0.6, 0.8 bps/Hz). In this case, we have set $\zeta = 0.8$ and $\alpha = 0.2$. For the comparison, DL transmission is also obtained using (27) of outage probability curves. As observed in Fig. 6, the CR-WBAN with the TSS protocol shows performance superiority compared to the DL transmission, particularly from the mid to SNR region. DL shows the transmission solely for three different target rates such as $R_p = 0.4$, 0.6, 0.8 bps/Hz. This improvement is attributed to the increased diversity gain achieved under the TSS protocol through the cooperative relaying link established. Additionally, it is evident that as the target rate R_p increases from 0.4 to 0.8 bps/Hz, it degrades the outage probability performance of the proposed CR-WBAN.

Figure 7 displays the outage probability performance vs SNR for the secondary communication when utilizing the TSS for $\alpha = 0.2$ value in the proposed CR-WBAN. In this plot, we showcase curves that represent diverse combinations of values for R_s and ζ. It is evident from Fig. 7 that the performance of OP for the secondary network reduces as the values of ζ and R_s increase. The outage probability of (35b) is provided for $N = 4$, and as the SNR increases, the OP performance is reduced. It is expected because as ζ increases, a larger portion of the available power is assigned to the primary signal, this results in a reduced amount of power available for secondary transmissions. Thus, the setup with R_s set to 0.8 bps/Hz and ζ set to 0.95 exhibits enhanced OP within the secondary communication network. Consequently, the secondary network experiences deteriorated OP performance due to the reduced power allocation for its transmission. Hence, a smaller ζ value is preferable to enhance the secondary communication performance.

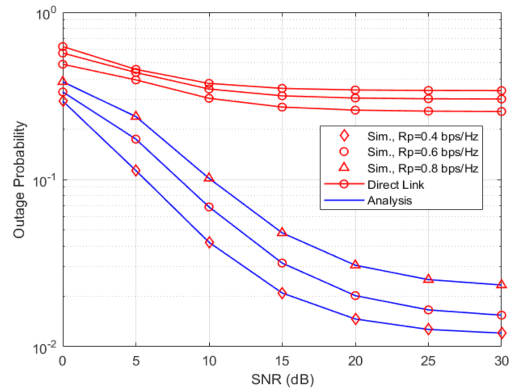

Fig. 6. OP vs SNR for TSS protocol in primary network.

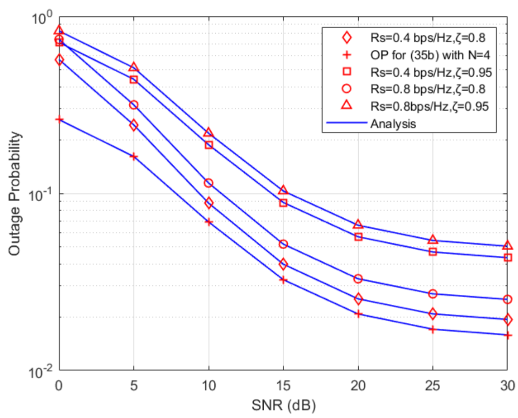

Fig. 7. OP vs SNR for TSS protocol in the secondary network.

Figure 8 shows the outage probability vs PSS parameter ρ primary network performance under diverse values of ζ and η_a. In this scenario, we set the target rate as $R_p = 0.8$ bps/Hz, resulting in an admissible range for ζ, which is $0.67 < \zeta < 1$. Based on the information presented in Fig. 8, we observe the existence of a critical value of ρ that minimizes the OP of the primary network. The critical value of ρ is found to be 0.43. To enable spectrum access cooperation, an effective value of $\zeta = 0.7$. It should be noted that the effective value of $\zeta = 0.7$ for the PSS protocol is relatively lower than that used for the TSS protocol.

Figure 9 depicts the OP vs SNR utilizing PSS protocol for the primary network. These curves are shown for diverse target rates such as $R_p = 0.4$, 0.6, and 0.8 bps/Hz for specific $\rho = 0.43$ and $\zeta = 0.8$. The primary network exhibits a substantial enhancement in outage probability performance when employing the PSS protocol relative to DL transmission. The DL curves represent direct transmission performance for three different target rates $R_p = 0.4$, 0.6, and 0.8 bps/Hz. This improvement is particularly noticeable in the mid to high SNR range. A comparative analysis reveals that the PSS protocol surpasses the TSS protocol in terms of OP under equivalent system parameters. This becomes especially apparent when observing the reduced SNR range.

Figure 10 represents the OP vs SNR for the secondary network employing the PSS protocol. The plots are shown for different combinations of values of R_s and ζ, with the parameter $\rho = 0.43$. Analyzing the information represented in Fig, 10, it becomes apparent that with the escalation of R_s

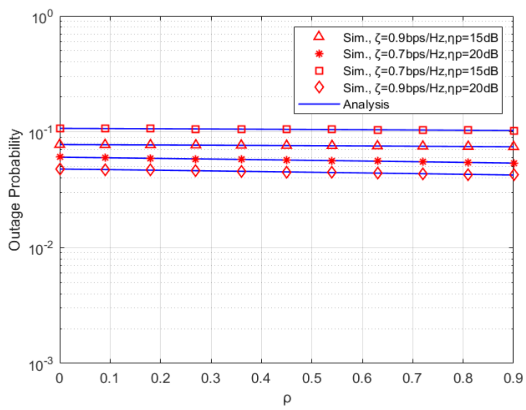

Fig. 8. OP vs ρ for PSS protocol in the primary network.

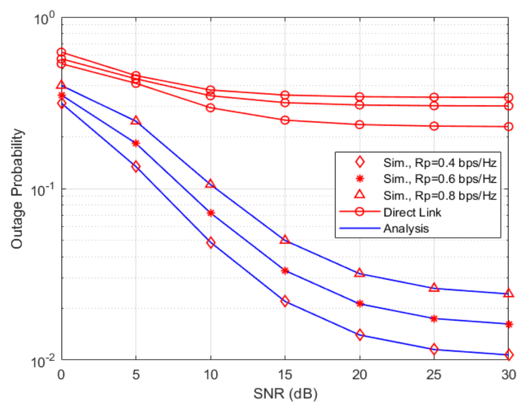

Fig. 9. OP vs SNR for PSS protocol in the primary network.

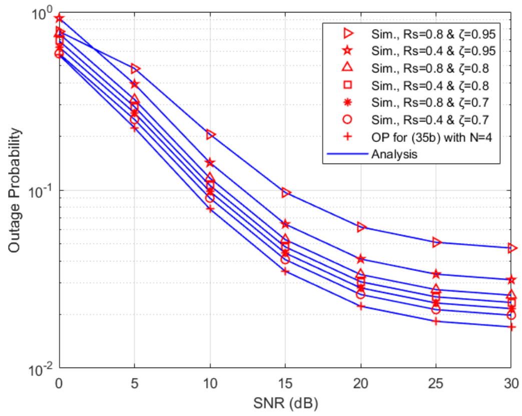

Fig. 10. OP vs SNR for PSS protocol in the secondary network.

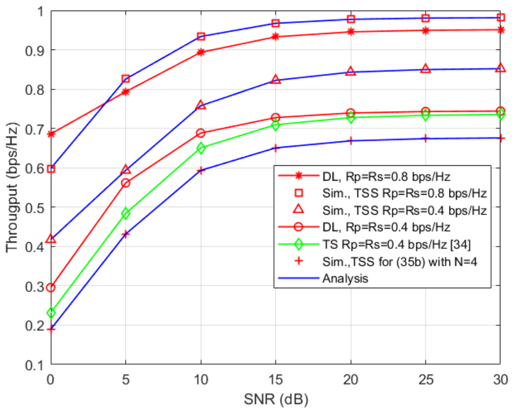

(a)

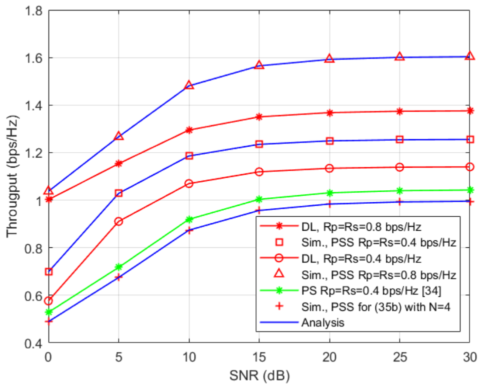

(b)

Fig. 11. (a) Throughput of TSS protocol; (b) Throughput of PSS protocol CR-WBAN.

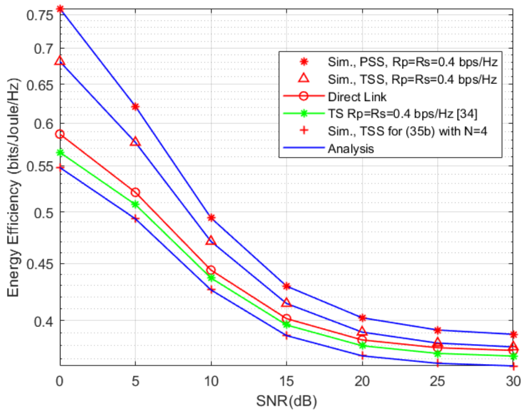

(a)

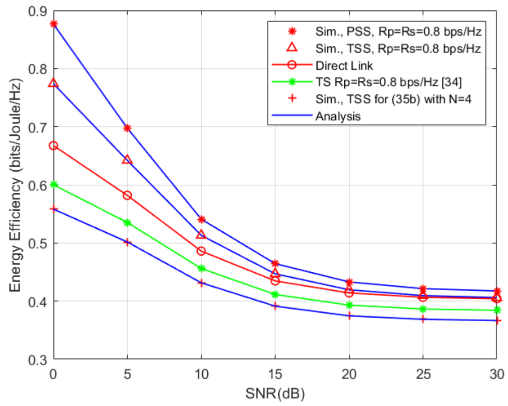

(b)

Fig. 12. (a) Energy efficiency with $R_p = R_s = 0.4$ bps/Hz; (b) Energy efficiency with $R_p = R_s = 0.8$ bps/Hz of CR-WBAN.

and ζ values, OP of the secondary network tends to reduce based on the increasing parameter values (R_s & ζ). The outage probability of the PSS protocol for (35b) is given for $N = 4$, and as the SNR increases, the OP decreases. However, Figure 10 shows that the secondary network's performance has improved when using the PSS protocol in comparison to the TSS protocol. The observed discrepancy can be ascribed to the reduced efficacy of the spectrum access factor ζ under the PSS protocol.

In Fig. 11, taking into account both the TSS and PSS protocols, we examine the system throughput performance within the CR-WBAN. This evaluation encompasses parameter values of $R_p = R_s = 0.4$ and 0.8 bps/Hz. We employ a critical value of $\alpha = 0.2$ under TSS protocol, resulting in an effective value of $\zeta = 0.53$ when $R_p = 0.4$ bps/Hz, and $\zeta = 0.78$ when $R_p = 0.8$ bps/Hz. Comparably, we set the critical value for PSS protocol at $\rho = 0.43$, resulting in an effective value of $\zeta = 0.45$ for $R_p = 0.4$ bps/Hz, and $\zeta = 0.7$ for $R_p = 0.8$ bps/Hz. A comparative analysis with a two-way relaying protocol [34] is also conducted. It is evident that when the SNR increases noticeably, the throughput tends to approach its maximum value. Furthermore, it is evident that the performance of throughput in the PSS protocol notably outperforms the TSS protocol across the entire SNR range and even surpasses the throughput of the DL particularly in the high SNR.

Figures 12a and 12b represent the energy efficiency vs SNR for the CR-WBAN system incorporating both the TSS and PSS protocols at two sets of target rates: $R_p = R_s = 0.4$ bps/Hz and 0.8 bps/Hz. If the same values for α, ρ, and ζ are established for both the TSS and PSS protocols then the comparison between the two protocols in aspects of energy efficiency will be more reliable. Both the TSS and PSS protocols outperform the DL transmission in aspects of energy efficiency. Moreover, the PSS system demonstrates greater energy efficiency when contrasted with the TSS system. Indeed, the observation of SNR increases the energy efficiency decreases significantly. This phenomenon occurs because, at increased SNR values, the through-

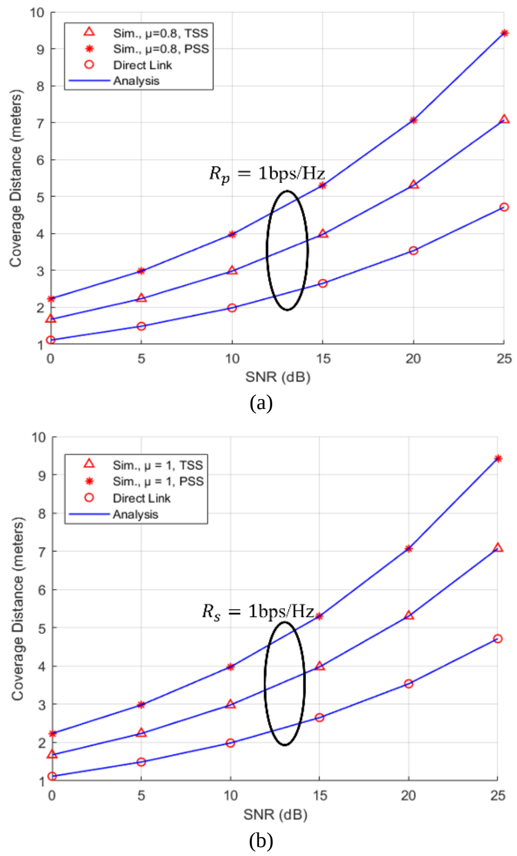

Fig. 13. (a) Coverage distance of the primary network; (b) Coverage distance of the secondary network of CR-WBAN.

put achieved becomes much less compared to the consumed power. Consequently, the network's energy efficiency reduces as a result of this imbalance between throughput and power consumption.

In Fig. 13a and 13b, the graphical representations illustrating the coverage distances of different schemes with parameters set at $R_p = R_s = 1$ bps/Hz for both PSS and TSS, $\mu = 0.8$ for the primary network and $\mu = 1$ for a secondary network where $P_{out}(R_p) = P_{out}(R_s) = 0.1$. The probability of SNR enhancement changes based on the proposed scheme, and the analytical result perfectly corresponds with the results from simulations results. According to the proposed system, the coverage yields better results for the PSS system in comparison to the TSS system, even when both operate with the same value. This is evident that the scheme being examined offers superior cell coverage in comparison to direct transmission without the utilization of spectrum access, regardless of the value R_p and R_s. The clear observation is that our proposed scheme can extend spectrum coverage and simultaneously enhance link reliability, in contrast to direct transmission.

5. Conclusion and Future Work

We studied an investigation on energy harvesting-based CR-WBAN where both primary communication and secondary networks are considered in the human body. The study focuses on employing cooperative spectrum access for these communications. This evaluation takes into account the impact of fading channels following a log-normal distribution. The energy harvesting ratio within the time switching and the power splitting are examined through numerical investigation. The system performance was assessed in aspects of outage probability for primary and secondary networks, throughput, energy efficiency, and coverage analysis. The findings from our study demonstrate that the PSS protocol significantly excels the TSS protocol, thereby enabling spectrum access communication within the CR-WBAN. Additionally, the coverage analysis shows that the proposed system demonstrates superior performance in both the PSS and TSS protocols. In our future research, we will aim to address energy-constrained nodes by proposing a two-way cooperative communication RIS-WBAN with EH. The signal quality and efficiency of data transmission between body sensors and external devices can be improved, while also reducing energy consumption. This is particularly important for battery-powered wearable devices, extending their operational life and enhancing reliability in real-time health monitoring systems. In the two-way cooperation communication, we will explore how PSS and TSS can facilitate bidirectional information exchange between two nodes, enabling them to transmit and receive data simultaneously and also implement in the context of Multiple-Input Multiple-Output (MIMO) and Non-Orthogonal Multiple Access (NOMA) systems.

Appendix A: Proof of Theorem 1

Using (7), the CDF $F_{\gamma_{adb}}(x) = \Pr[\gamma_{adb} < x]$ is evaluated, for $x < \zeta / (1 - \zeta)$, as

$$F_{\gamma_{adb}}(x) = \Pr\left[\gamma_{ad} < \frac{x\left(1+\zeta\beta_2\left|h_{db}\right|^2\right)}{\beta_1\left(\zeta-(1-\zeta)x\right)\left|h_{db}\right|^2}\right] \triangleq \phi(x). \quad (40)$$

And otherwise, for $x \geq \zeta / (1 - \zeta)$, it is unity. Which is evaluated as

$$\phi(x) = \int_0^\infty F_{\gamma_{ad}}\left(\frac{x(1+\zeta\beta_2 y)}{\beta_1(\zeta-(1-\zeta)x)y}\right)F_{|h_{db}|^2}(y)\,\mathrm{d}y. \quad (41)$$

Upon substituting the CDF of γ_{ad} and PDF of $|h_{db}|^2$ expressions from (23) and (22), respectively, into (41), we arrive at the result presented in (31).

Appendix B: Proof of Theorem 2

The CDF $F_{\gamma_{adc}}(x)$ is expressed using (32) as

$$F_{\gamma_{adc}}(x) = \Pr\left[\gamma_{ad} < \frac{x\left(1+\zeta\beta_1\left|h_{dc}\right|^2\right)}{(1-\zeta)\beta_2\left|h_{dc}\right|^2}\right] \quad (42)$$

which can be determined to be

$$F_{\gamma_{\mathrm{adc}}}\left(x\right)=\int_{0}^{\infty}F_{\gamma_{\mathrm{ad}}}\left(\frac{x\left(1+\zeta\beta_{1}y\right)}{\left(1-\zeta\right)\beta_{2}y}\right)F_{\left|h_{\mathrm{dc}}\right|^{2}}\left(y\right)\mathrm{d}y. \tag{43}$$

Upon applying the CDF of γ_{ad} and PDF of $|h_{\mathrm{dc}}|^2$ from (23) and (22), respectively, to (43), we arrive at the result presented in (35a) and (35b).

References

[1] KHASAWNEH, M., AZAB, A., ALRABAEE, S., et al. Convergence of IoT and cognitive radio networks: A survey of applications, techniques, and challenges. *IEEE Access,* 2023, vol. 11, p. 71097–71112. DOI: 10.1109/ACCESS.2023.3294091

[2] QADRI, Y. A., NAUMAN, A., ZIKRIA, Y. B., et al. The future of healthcare internet of things: A survey of emerging technologies. *IEEE Communications Surveys & Tutorials,* 2020, vol. 22, no. 2, p. 1121–1167. DOI: 10.1109/COMST.2020.2973314

[3] SALAYMA, M., AL-DUBAI, A., ROMDHANI, I., et al. Wireless body area network (WBAN): A survey on reliability, fault tolerance, and technologies coexistence. *ACM Computing Surveys (CSUR),* 2018, vol. 50, no. 3, p. 1–38. DOI:10.1145/3041956

[4] LI, S., YANG, H. C., XU, F., et al. Energy-efficient relay transmission for WBAN: Energy consumption minimizing design with hybrid supervised/reinforcement learning. *IEEE Internet of Things Journal,* 2024, vol. 11, no. 10, p. 17770–17779. DOI: 10.1109/JIOT.2024.3361772

[5] PREETHICHANDRA, D. M. G., PIYATHILAKA, L., IZHAR, U., et al. Wireless body area networks and their applications—a review. *IEEE Access,* 2023, vol. 11, p. 9202–9220. DOI: 10.1109/ACCESS.2023.3239008

[6] GHOSH, B., ADHIKARY, S., CHATTOPADHYAY, S., et al. Achieving energy efficiency and impact of SAR in a WBAN through optimal placement of the relay node. *Wireless Personal Communications,* 2023, vol. 130, p. 1861–1884. DOI: 10.1007/s11277-023-10361-z

[7] TALEB, H., NASSER, A., ANDRIEUX, G., et al. Energy consumption improvement of a healthcare monitoring system: application to LORAWAN. *IEEE Sensors Journal,* 2022, vol. 22, no. 7, p. 7288–7299. DOI: 10.1109/JSEN.2022.3150716

[8] OLATINWO, D. D., ABU-MAHFOUZ, A. M., HANCKE, G. P., et al. Energy efficient priority-based hybrid mac protocol for IoT-enabled WBAN systems. *IEEE Sensors Journal*, 2023, vol. 23, no. 12, p. 13524–13538. DOI: 10.1109/JSEN.2023.3273427

[9] CAVALLARI, R., MARTELLI, F., ROSINI, R., et al. A survey on wireless body area networks: Technologies and design challenges. *IEEE Communications Surveys & Tutorials,* 2014, vol. 16, no. 3, p. 1635–1657. DOI: 10.1109/SURV.2014.012214.00007

[10] ZHUMAYEVA, M., DAUTOV, K., HASHMI, M., et al. Wireless energy and information transfer in WBAN: A comprehensive state-of-the-art review. *Alexandria Engineering Journal,* 2023, vol. 85, p. 261–285. DOI: 10.1016/j.aej.2023.11.030

[11] ALI, H., RIAZ, M., BILAL, A., et al. Comparison of energy harvesting techniques in wireless body area network. *International Journal of Multidisciplinary Sciences and Engineering,* 2016, vol. 7, no. 6, p. 20–24. ISSN: 2045-7057

[12] GUO, W., HOU, Y., GAN, Y., et al. Efficient data transmission mechanisms in energy harvesting wireless body area networks: A survey. *Computer Networks,* 2024, vol. 254, p. 1–31. DOI: 10.1016/j.comnet.2024.110769

[13] CHAUDHARY, S., AGARWAL, A., MISHRA, D., et al. Enhancing longevity: Sustainable channel modeling for wireless-powered implantable bans. *Ad Hoc Networks,* 2024, vol. 163, p. 1–10. DOI: 10.1016/j.adhoc.2024.103584

[14] HU, J., XU, G., HU, L., et al. A cooperative transmission scheme in radio frequency energy-harvesting WBANs. *Sustainability,* 2023, vol. 15, p. 1–13. DOI: 10.3390/su15108367

[15] PADHY, A., JOSHI, S., BITRAGUNTA, S., et al. A survey of energy and spectrum harvesting technologies and protocols for next generation wireless networks. *IEEE Access,* 2020, vol. 23, no. 9, p. 1737–1769. DOI: 10.1109/ACCESS.2020.3046770

[16] HUANG, X., SHAN, H., SHEN, X. On energy efficiency of cooperative communications in wireless body area network. In *IEEE Wireless Communications and Networking Conference.* Cancun (Mexico), 2011, p. 1097–1101. DOI: 10.1109/WCNC.2011.5779313

[17] TRAN, L. C., MERTINS, A., HUANG, X., et al. Comprehensive performance analysis of fully cooperative communication in WBANs. *IEEE Access,* 2016, vol. 4, p. 8737–8756. DOI: 10.1109/ACCESS.2016.2637568

[18] LI, S., HU, F., MAO, Z., et al. Sum-throughput maximization by power allocation in WBAN with relay cooperation. *IEEE Access,* 2019, vol. 7, p. 124727–124736. DOI: 10.1109/ACCESS.2019.2938331

[19] MOSAVAT-JAHROMI, H., MAHAM, B., TSIFTSIS, T. A. Maximizing spectral efficiency for energy harvesting-aware WBAN. *IEEE Journal of Biomedical and Health Informatics,* 2016, vol. 21, no. 3, p. 732–742. DOI: 10.1109/JBHI.2016.2536642

[20] GURJAR, D. S., SINGH, U., UPADHYAY, P. K. Energy harvesting in hybrid two-way relaying with direct link under Nakagami-m fading. In *IEEE Wireless Communications and Networking Conference (WCNC).*Barcelona (Spain), 2018, p. 1–6. DOI: 10.1109/WCNC.2018.8377371

[21] LI, S., HU, F., MAO, Z., et al. Joint power allocation for energy harvesting to maximize throughput in classified WBAN. In *IEEE Global Communications Conference (GLOBECOM).* Waikoloa (HI, USA), 2019, p. 1–6. DOI: 10.1109/GLOBECOM38437.2019.9013828

[22] LIU, L., ZHANG, R., CHUA, K. C. Wireless information and power transfer: A dynamic power splitting approach. *IEEE Transactions on Communications,* 2013, vol. 61, no. 9, p. 3990–4001. DOI: 10.1109/TCOMM.2013.071813.130105

[23] HU, F., LIU, X., SUI, D., et al. Performance analysis of reliability in wireless body area networks. *IET Communications,* 2017, vol. 11, no. 6, p. 925–929. DOI: 10.1049/iet-com.2016.0997

[24] ALKHAYYAT, A., JAWAD, S. F., SADKHAN, S. B. Cooperative communication based: Efficient power allocation for wireless body area networks. In *The 1st AL-Noor International Conference for Science and Technology (NICST).* Sulimanyiah (Iraq), 2019, p. 106–111. DOI: 10.1109/NICST49484.2019.9043843

[25] SODAGARI, S., BOZORGCHAMI, B., AGHVAMI, H. Technologies and challenges for cognitive radio enabled medical wireless body area networks. *IEEE Access,* 2018, vol. 6, p. 29567 to 29586. DOI: 10.1109/ACCESS.2018.2843259

[26] HAN, Y., PANDHARIPANDE, A., TING, S. H. Cooperative decode-and-forward relaying for secondary spectrum access. *IEEE Transactions on Wireless Communications,* 2009, vol. 8, no. 10, p. 4945–4950. DOI: 10.1109/TWC.2009.081484

[27] GHOSH, S., ACHARYA, T., MAITY, S. P. Outage analysis in SWIPT enabled cooperative AF/DF relay assisted two-way spectrum sharing communication. *IEEE Transactions on Cognitive Communications and Networking,* 2022, vol. 8, no. 3, p. 1434–1443. DOI: 10.1109/TCCN.2022.3171223

[28] ZHANG, C., GE, J., LI, J., et al. A unified approach for calculating the outage performance of two-way AF relaying over fading

channels. *IEEE Transactions on Vehicular Technology,* 2014, vol. 64, no. 3, p. 1218–1229. DOI: 10.1109/TVT.2014.2329853

[29] YANG, L., ALOUINI, M. S., QARAQE, K. On the performance of spectrum sharing systems with two-way relaying and multiuser diversity. *IEEE Communications Letters,* 2012, vol. 16, no. 8, p. 1240–1243. DOI: 10.1109/LCOMM.2012.052112.120746

[30] SHUKLA, A, K., UPADHYAY P, K., SRIVASTAVA, A., et al. Enabling co-existence of cognitive sensor nodes with energy harvesting in body area networks. *IEEE Sensors Journal,* 2021, vol. 21, no. 9, p. 11213–11223. DOI: 10.1109/JSEN.2021.3062368

[31] NASIR, A. A., ZHOU, X., DURRANI, S., et al. Relaying protocols for wireless energy harvesting and information processing. *IEEE Transactions on Wireless Communications,* 2013, vol. 12, no. 7, p. 3622–3636. DOI: 10.1109/TWC.2013.062413.122042

[32] SUI, D., HU, F., ZHOU, W., et al. Relay selection for radio frequency energy-harvesting wireless body area network with buffer. *IEEE Internet of Things Journal,* 2018, vol. 5, no.2, p. 1100 to 1107. DOI: 10.1109/JIOT.2017.2788207

[33] LIU, Y., DING, Z., ELKASHLAN, M., et al. Cooperative non-orthogonal multiple access with simultaneous wireless information and power transfer. *IEEE Journal on Selected Areas in Communications,* 2016, vol. 34, no. 4, p. 938–953. DOI: 10.1109/JSAC.2016.2549378

[34] TUNG, N. T., NAM, P. M., TIN, P. T., et al. Performance evaluation of a two-way relay network with energy harvesting and hardware noises. *Digital Communications and Networks,* 2021, vol. 7, no. 1, p. 45–54. DOI: 10.1016/j.dcan.2020.04.003

About the Authors ...

Sree Nidhi SRINIVASAN (corresponding author) received the B.E. degree in Electronics and Communication Engineering in 2019, and M.E.-Applied Electronics degree from the Anna University in 2021. She is currently pursuing the Ph.D. degree in Anna University and working as Project Associate at SETS, Chennai. Her Ph.D. topic is in the field of wireless body area networks and she is proposing security and energy harvesting protocols for wireless body area networks. Her research interests are in wireless communication networks, which includes wireless body area networks, wireless sensor networks, cognitive radio, energy efficient communication, reliable scheduling, and QoS provisioning in wireless networks.

Pavithra SURESH KUMAR received the B.E. degree in Electronics and Communication Engineering from Indira Institute Engineering and Technology Thiruvallur and M.E. degree in Applied Electronics at Anna University CEG campus, Chennai, India, in 2019 and 2023. She is currently working as a Senior Packaging engineer at Western Digital (SanDisk) company at Bangalore.

Sridharan DURAISAMY received the B.Tech. degree and the M.E. degree in Electronics Engineering from the Madras Institute of Technology, Anna University, Chennai, India, in 1991 and 1993, respectively, and the Ph.D. degree from the Faculty of Information and Communication Engineering, Anna University, in 2005. He is currently a Professor with the Department of Electronics and Communication Engineering, CEG Campus, Anna University. His current research interests include internet technology, network security, distributed computing, and wireless sensor networks. He was a recipient of the Young Scientist Research Fellowship by the Department of Science and Technology, SERC, Government of India.